published in Environmental Chemistry 16 (2019) 151-164

Assessment of labilities of metal complexes with the Dynamic Ion Exchange Technique

F. Quattrini[a], J. Galceran[a*], C. Rey-Castro[a], J. Puy[a], and C. Fortin[b]

[a]Departament de Química. Universitat de Lleida, and AGROTECNIO, Rovira Roure 191, 25198 Lleida, Catalonia, Spain

[b]Centre Eau Terre Environnement, Institut national de la Recherche Scientifique, 490 Rue de la Couronne, Quebec City, QC, G1K 9A9, Canada.

* corresponding author: galceran@quimica.udl.cat

Abstract

The Dynamic Ion Exchange Technique (DIET) is proposed to provide speciation information, which can be used to establish links with metal bioavailability in natural waters. The experimental setup consists of a few milligrams of a sulfonic acid type ion exchange resin packed in a plastic microcolumn and coupled to a peristaltic pump for a sample to interact with the resin which is afterwards eluted. The evolution of both, the accumulated moles in the resin and the concentration of the effluent, can provide information on the dissociation of different metal-ligand complexes in comparison with transport properties. This information can be converted into the lability degree of a given complex or the DIET concentration c_{DIET}, which accounts for the labile fraction contributing to the metal accumulation by the resin column at the operation conditions. c_{DIET} can be extended to columns containing chelating resins (such as those with Chelex) or to chromatography. A comprehensive modelling of the involved phenomena (such as diffusion, advection, reaction kinetics and electrostatic partitioning) leads to the quantitative interpretation of accumulation time series (accumulation curves) or effluent evolution (breakthrough curves). Particularly simple analytical expressions can be used for short exposure times, when a (quasi) steady-state is attained. These models have been checked against results from complexes of Cu and Ni with ligands such as ethylenediamine, ethylenediaminetetraacetic, iminodiacetic, glutamic, salicylic, malonic and malic acids, which yield complexes with varying charges. Caution is advised when estimating the free metal fraction from DIET measurements, as c_{DIET} and the free metal concentration can be considered to be equal only in the case of extremely inert complexes.

Keywords: trace metal speciation, availability, ion exchange columns

1. Introduction

Metal speciation provides crucial information for current paradigms of ecotoxicity (such as the Free Ion Activity (Anderson et al. 1978) and Biotic Ligand (Paquin et al. 2002) Models), and thus several techniques have been developed along the years for this purpose. Among the most recent ones, we can quote voltammetric techniques such as Absence of Gradients and Nernstian Equilibrium Stripping (Companys et al. 2017), membrane-based techniques such those using Polymer Inclusion Membranes (Companys et al. 2018;Vera et al. 2018), Donnan Membranes (Temminghoff et al. 2000) and dialysis membranes (Berggren 1989;Franklin et al. 2007), as well as techniques based on functionalised resins (Alberti et al. 2007;Pesavento et al. 2009;Sunda 1984;Tantra et al. 2016). Among the latter, special mention must be made of the Ion Exchange Technique (IET), developed by Cantwell (Cantwell et al. 1982) and later applied by many others, including Campbell and Fortin (Crémazy et al. 2015;Fortin and Campbell 1998). IET is a column equilibration technique that consists of an accumulation step, where the sample solution is flushed through a column packed with a sulphonic acid type resin until equilibrium is attained. An elution step follows, then the accumulated metal is measured with a suitable elemental analysis technique. This amount can, then, be related to the corresponding free metal concentration in solution *via* a conditional exchange constant determined by calibrating the system in the conditions of interest.

The knowledge acquired with all the aforementioned techniques is related only to the thermodynamic aspects of the systems studied and, though valuable, in several cases is too limited (Zhao et al. 2016). Dynamic speciation aims at providing information beyond thermodynamics, such as rates of association/dissociation and mobility. In the case of the DGT (Diffusive Gradients in Thin films) passive sampler (Davison 2016), as in many others, a flux is measured and interpreted as a surrogate of the supply from the medium

to the organism, which leads to the determination of c_{DGT}, a kind of effective metal concentration or "labile fraction".

Recent work (Leguay et al. 2016;Nduwayezu et al. 2016;Rowell et al. 2018) has considered the possibility of extracting meaningful information from the time-resolved accumulations in IET columns (that we label as "accumulation curves"). In this new approach, called Dynamic Ion Exchange Technique (DIET), the moles of metal accumulated by the resin (n_{acc}) is recorded as a function of contact time, before equilibrium is reached (see Fig 1a). One could consider DIET as a way of exploiting an early regime (Peijnenburg et al. 2014) in the accumulation curve (see Fig 1b). The initial slope of the accumulation curve (labelled as "accumulation rate", R_{acc}) has been assumed to be related to the free metal concentration in the sample *via* an empirical relationship (Nduwayezu et al. 2016). In those cases where the effluent concentration is above the quantification limit of the analytical technique, the breakthrough curves (see Fig 1c) can also be recorded, to obtain additional information. The main advantage of DIET over IET is that it is much more economical both in terms of time and sample volume, as it does not require waiting for the full attainment of equilibrium. This can become critical when equilibration is particularly slow, as in the case of highly charged ions (Leguay et al. 2016) or at low ionic strengths. Although the first results seemed promising, it is still unclear whether the accumulation rate actually reflects only the binding of free metal ion or if the labile species contribute as well (Nduwayezu et al. 2016).

Dynamic speciation (van Leeuwen et al. 2005) has been rarely tackled with columns (Alvarez et al. 2004;Bowles et al. 2006;Figura and Mcduffie 1980;Procopio et al. 1997;Wen et al. 2006), perhaps due to a limited interpretative framework. Most work has just relied on semi-empirical fractionation schemes. In general, the recovered fractions of metal reported in literature have been defined operationally, without the support of a

theoretical relationship with the thermodynamic, kinetic and transport properties of the different metal species present in the sample. In addition, in most of these cases, the sorbent materials are weakly acidic, chelating resins like Chelex 100 (iminodiacetic functional groups) (Herrin et al. 2001), while little information is found about strongly acidic, ion-exchange resin like Dowex (sulphonate functional groups).

For this reason, the purpose of this work is to interpret DIET via a comprehensive modelling approach, so that information on the kinetic properties of the complexes can be retrieved. Four models are presented (and derived in detail in the Supporting Information, SI) to describe accumulation either by an individual bead or by the column as a whole, either in steady state (SS) or under transient conditions (see Table 1). From the entire modelling exercise, it emerges that Model IV is the most useful for practical purposes, because it describes the early stage experimental data with very simple analytical expressions (see section 3.5.2). The DIET-labile concentration (c_{DIET}) is defined in section 3.6 and practical formulas to compute it are proposed in section 3.8.

2. Materials and Methods

2.1 Equipment and Reagents

The medium for all of the experiments has the major ion composition of a typical algal growth medium (Ca(II): 6.8×10^{-5} mol L^{-1}; Mg(II): 8.12×10^{-5} mol L^{-1}; K(I): 4.22×10^{-3} mol L^{-1}; all the cations were introduced as nitrate salts), as given in (Fortin and Campbell 2001). In all of the experiments the pH was fixed at 6.0 with 1×10^{-3} mol L^{-1} 2-(N-morpholino)ethanesulfonic acid (MES). The total ionic strength of the medium was I=4.4×10^{-3} mol L^{-1}. The concentrations of the competing ligands were chosen so as to have clearly different values of the free metal fraction of Cu or Ni, as computed with the speciation software Visual MINTEQ (Gustafsson 2016). Details on the reagents and equipment are provided in the SI. The ligands chosen were ethylenediamine (en),

ethylenediaminetetraacetic (EDTA), iminodiacetic (IDA), glutamic, salicylic, citric, malonic and malic acids.

2.2 Column preparation and use

Three different types of the strongly acidic cation exchange Dowex 50 sulphonic resin were used (nominal values):

- Dowex 50x2 200-400 mesh (38-75 µm) – crosslinking degree of 2%, 0.6 meq. mL^{-1} capacity.
- Dowex 50x4 100-200 mesh (75-150 µm) – crosslinking degree of 8%, 1.1 meq. mL^{-1} capacity.
- Dowex 50x8 50-100 mesh (150-300 µm) - crosslinking degree of 8%, 1.7 meq. mL^{-1} capacity.

The experimental setup was similar to a standard IET experiment (Fortin and Campbell 1998) and is schematized in Fig 1a. A known amount of resin was packed in a plastic microcolumn. The resin was then cleaned (with 1.5 mol L^{-1} HNO_3 acid, 0.1 mol L^{-1} KOH and ultrapure water) and conditioned by flushing a solution identical to the sample background (with no trace metals or ligands), until the pH and ionic strength of the eluate were the same as those at the inlet. In our conditions, stabilisation of the pH required about 20 min. The sample itself was, then, passed through the column for different periods of time (*e.g.* 5-10-30 min.). After each period, the resin was eluted with 1.5 mol L^{-1} HNO_3 at 0.5 mL min^{-1} for 20 min and the eluate was collected; the column was renewed and reconditioned, and a new run was started. Unless otherwise specified, the samples were flushed at 4.5 mL min^{-1}; the flow rate was checked periodically since the tubing tended to deteriorate over time.

The metal uptake can also be followed by measuring the metal concentration in the effluent during the initial pumping of the test solution through the column, instead of eluting the metal accumulated in the beads.

2.3 Concentration measurements

All the sample aliquots were acidified to 1% HNO_3. Those from the highly acidic eluates had to be diluted accordingly before analysis. All the samples were analysed with ICP-OES (Horiba Jobin Yvon) or ICP-MS (Agilent 7700x).

3. Interpretation of experimental results

3.1 Accumulation curves

The purpose of this section is the description of the experimental data obtained with DIET in synthetic solutions. First, the plots of metal accumulations in the column *vs*. time (*i.e*. accumulation curves) such as those presented in Fig 2 (for a fixed amount of total metal and variable amounts of ligands) were analysed.

In general, four different kinds of accumulation curves were distinguished. First (Fig 2a), systems for which the metal accumulates in the column following a linear trend over time, with a slope (R_{acc}) equal to that of the ligand-free metal solutions. The behaviour of this type of systems indicates (*i*) a high rate of dissociation within the column and (*ii*) conditions far away from equilibrium of the solution with the resin (*i.e.*, far from the maximum capacity of the resin).

Second (Fig 2b), there are other systems that display accumulation curves where R_{acc} approaches the value observed in the absence of ligands at short exposure times, but it soon decays while the accumulation tends to a constant value, indicative of resin-sample equilibrium. Depending on the lability of the metal complexes and the extent of the buffering of the free metal ion, the rate of metal binding may vary, as can be seen in the case of the Cu-malate complexes: with an increase of the ligand concentration from

1.5×10^{-4} mol L^{-1} to 5×10^{-3} mol L^{-1}, the time to attain equilibrium may decrease from several hours to a few minutes.

Third (Fig 2c), there are systems that show linear accumulation curves with a slope (R_{acc}) smaller than that obtained with the ligand-free metal solutions (at the same total metal concentration). This indicates that R_{acc} is not strictly proportional to the total concentration in all cases. In fact, the analysis of data obtained at varying ligand-to-metal ratios in these systems shows a monotonic trend of R_{acc} with the concentration of free metal ion (see also the Ni-EDTA data in Fig 3). Therefore, a question arises as to whether R_{acc} depends exclusively on the value of the free metal ion concentration in the bulk sample (Nduwayezu et al. 2016) or, rather, it reflects the effective rate of dissociation of the metal complexes inside the resin column. In the latter case, DIET results would allow us to obtain information on the labile or inert character of the complexes (*i.e.*, the *dynamic* speciation).

Finally, a fourth kind of system, typically under ligand excess conditions and very low free metal concentration (*e.g.*, Cu-malate at the highest ligand concentration, shown in Fig 2d) exhibits a constant (and very small) accumulation at all times, which is the result of an almost instantaneous attainment of resin-sample equilibrium. In these cases, no information on the dissociation kinetics can be obtained.

3.2 Evolution of effluent concentrations

As done for the accumulation curves in the previous section, the breakthrough curves, like those shown in Fig 4b, can also be characterised. Note that equilibrium between the resin and the metal ions in solution is reached when the metal accumulation in the resin (Fig 4a) no longer increases with time and the effluent concentration $c_{T,M}^{eff}$ reaches the input concentration $c_{T,M}$ (indicated by the horizontal dashed line in Fig 4b).

The two series with citrate complexes show that equilibrium has been practically reached after 10 minutes of exposure. The shape of the curve of Ni in absence of ligand obtained with the small resin beads (red ×; Fig 4b) illustrates another characteristic behaviour where the effluent concentration rises up slowly to the input value $c_{T,M}$, resulting in a low slope. The shape of the curve of Ni in absence of ligand obtained with the larger resin (blue *) is another typical example of the systems studied in this work: it exhibits an initial sudden increase followed by a stabilization, the "plateau". This plateau may reach an effluent concentration $c_{T,M}^{eff}$ that is slightly lower than the input concentration. In these conditions, the observed plateau could be misinterpreted as an indication that equilibrium between the resin and the metal in solution was reached, whereas, in fact, metal ions are still accumulating on the resin as showed in Fig 4a. This "biphasic" behaviour (fast increase followed by slow increase) has been previously reported in the literature (*e.g.* Fig 1 to 3 in (Nduwayezu et al.), Fig 1 in (Pesavento et al. 2010) or Figs 1b and S2 in (Leguay et al. 2016)) and it will be interpreted here in terms of a "steady state plateau", for reasons discussed in section 3.7.

3.3 Modelling of DIET. General assumptions.

To start with the essential component, model I considers just the accumulation by one bead in contact with the sample and its evolution from the initial stages until equilibrium. It will be shown in section 3.4 that the transient stage before SS is short, so that SS can be safely assumed (model II). A "diffusional" SS regime towards a particular bead is applied later on to the column models III and IV. The next modelling step is to consider all the beads in the whole column: either following the time evolution (model III) or just concentrating in the global steady state (model IV). The advantage of SS models is that simple analytical expressions can be derived (see Table 1). Model IV can be proposed as the *de facto* model for DIET. In all models, the metal (M) reacts with a ligand (L) to

produce a complex with stoichiometry 1:1 (ML). Their charges are z_M (+2 for the metal ions studied here), z_L and z_{ML}, where:

$$z_{ML} = z_M + z_L \quad (1)$$

These charges are usually omitted in the notation of the species for the sake of simplicity (the SI contains a complete list of nomenclature).

As confirmed by the similitude of the accumulation curves of Ni and Cu, the binding of the metal ions to a strong acid cation exchange resin like Dowex can be assumed to be essentially electrostatic (for a description of the binding mechanism in chelating resins such as Chelex see *e.g.* (Quattrini et al. 2017)). As a first approximation, we neglect the steric interactions that are known to affect metal binding (Fortin et al. 2010). The affinity relationship is described by an equilibrium Donnan model. The here-used Boltzmann factor χ is the ratio of equilibrium concentrations of monovalent ions in the resin and aqueous domains (*i.e.* we neglect activity corrections as a first approximation):

$$\chi = \frac{\tilde{c}_{\text{monovalent}}\left(r = r_0^-\right)}{c_{\text{monovalent}}\left(r = r_0^+\right)} \quad (2)$$

where r_0^- and r_0^+ indicate the positions adjacent to the bead surface in the resin and in the solution, respectively. This Boltzmann factor depends on the density of charges in the resin matrix and on the ionic strength, which in our experiments was essentially fixed by KNO_3.

If we assume instantaneous equilibrium at the bead surface, then the concentrations of a given species *j* (of charge z_j) across the resin-solution interface are related with each other through:

$$\tilde{c}_j\left(r = r_0^-\right) = \chi^{z_j} c_j\left(r = r_0^+\right) \quad (3)$$

A value χ=128 was obtained from the experimental partitioning of Cu(II) at equilibrium, and it was used for numerical simulations. The large values of χ imply that the trace metal

ion (with z_M =+2) is taken up by the resin matrix right from the initial stages of contact and depleted from the solution boundary layer, so that $c_M\left(r=r_0^+\right)\approx 0$. Eventually, bulk equilibrium between the resin domain and the feed solution will be reached, so that $c_M\left(r=r_0^+\right)=c_M$ (no superscript is added to indicate the bulk conditions of the sample or solution mixture prior to its introduction in the column) and the total metal concentration inside the bead will be $\chi^{z_M}c_M+\chi^{z_{ML}}c_{ML}$.

The charge of the complex is very relevant to its behaviour regarding the "penetration" inside the bead. Negatively charged complexes are excluded from the resin matrix (Mongin et al. 2011;Puy et al. 2014), whereas the positively charged complexes show enhancement. At equilibrium, for z_M=+2 and z_{ML}=0, the expected amount of accumulated complexes relative to the total metal accumulated in the resin is negligible, since they are neutral. Even if these complexes can penetrate into the resin, they do not significantly concentrate inside (because $c_{ML}\left(r=r_0^-\right)=c_{ML}\left(r=r_0^+\right)$), contrary to the metal ion.

The lability of the complexes (of any charge), however, does have an impact in speeding up the overall metal uptake kinetics. As a quantifier of lability, we introduced the lability degree ξ (Galceran et al. 2001;Puy and Galceran 2017), defined as the ratio of the contribution of a complex to the metal flux over the maximal possible contribution. For inert complexes ξ=0, whereas ξ=1 for fully labile ones. Complexes can act as more or less labile depending on the analytical technique applied, the characteristics of the sensor or the composition of the sample.

Other common assumptions shared by the four models are:

1.- The supply to an individual resin bead results from diffusion in spherical geometry. The beads are spheres of fixed radius r_0. Diffusion in the solution surrounding the bead extends just to a finite distance r_1, defining a diffusion layer of effective thickness δ.

2.- Given that none of the complexes studied here are macromolecular, all metal species have a similar diffusion coefficient D_M (the same value in solution as inside the bead).

3.- Penetration of the different metal species inside the beads is allowed. In time-dependent models, all species penetrate according to their charge. In steady-state models (II and IV), the penetration of some species is neglected.

4.- There is instantaneous equilibrium at the bead surface, so that the partitioning Eqn. (3) applies.

5.- In the reaction:

$$\mathrm{M+L} \underset{k_d}{\overset{k_a}{\rightleftharpoons}} \mathrm{ML} \tag{4}$$

there is an excess of ligand, so that the concentrations of free ligand in solution (c_L if $r > r_0$) and inside the bead ($\tilde{c}_L$ if $r < r_0$) are constant over time or space (for both resin and solution domains).

The conditional (excess) stability constant (or coefficient) in solution is defined as:

$$K' = \frac{c_{ML}}{c_M} = \frac{k_a c_L}{k_d} \tag{5}$$

where k_a and k_d are the association and dissociation rate constants in solution, respectively.

3.4 Individual bead models

3.4.1 Time-dependent model of metal uptake by individual beads (Model I)

Model I considers null concentrations both in the solution diffusion boundary layer and within the resin at t=0 and it has the following boundary conditions: $c_{ML}(r_1, t) = c_{ML}$ and $c_M(r_1, t) = c_M$. Details on the model, its numerical resolution and code are given in the SI.

It was observed that, after a short transient period (less than half a second), the simulated uptake practically reaches SS (data not shown).

3.4.2 Steady state model of metal uptake by individual beads (Model II)

Model II assumes SS in order to reproduce the accumulation during the initial stages of uptake. A further simplification of Model II is that the surface of the bead acts as a perfect sink for the diffusion of M in solution, because of the large concentration jump at the bead surface (with a partitioning coefficient χ^{z_M}). This hypothesis is valid as long as the accumulation in the bead is far from equilibrium. The assumption of perfect sink conditions and mass transport limited by diffusion in the boundary layer around the beads has been shown to hold during the initial stages of metal uptake in batch experiments with Chelex resins (Quattrini et al. 2017) and is the operation principle of the DGT.

At SS, the flux *J* can be computed as (Buffle et al. 2007;Galceran et al. 2001;Galceran et al. 2003):

$$J = \frac{D_M\left(1+K'\xi\right)}{\delta} c_M \tag{6}$$

with:

$$\delta \equiv \frac{r_0}{r_1}\left(r_1 - r_0\right) \tag{7}$$

The next subsections detail the values of the lability degree to be used in Eqn. (6) for the different possible charges of the metal complexes.

3.4.2.1 Neutral complexes

Neutral complexes (with partitioning factor χ^0=1) can penetrate inside the beads. Given that at relatively short times (but once SS has been attained) the existing amounts of M and ML inside the beads are far from equilibrium with each other, we assume that there is no back-association of M and L inside the resin, but just dissociation of ML. Under excess ligand conditions, the metal contribution from complex dissociation inside the bead will be very relevant. This is similar to the treatment of penetration in several DGT

models (Mongin et al.2011;Puy et al. 2014;Uribe et al. 2011) where the accumulation is essentially due to this dissociation inside the resin.

As shown in the SI, the lability degree can be computed as:

$$\xi = 1 - \frac{1+K'}{K' + \frac{r_0(r_1-r_0)}{r_1 m}\coth\left(\frac{r_1-r_0}{m}\right) + \frac{r_1-r_0}{r_1} + \frac{r_0(r_1-r_0)(1+K')\chi^{z_{ML}}}{r_1\lambda}\coth\left(\frac{r_0}{\lambda}\right)} \quad (8)$$

with:

$$\lambda = \sqrt{\frac{D_{ML}}{k_d}} \quad (9)$$

and:

$$m = \sqrt{\frac{D_{ML}}{k_d + k_a c_L}} \quad (10)$$

k_a and k_d might differ from the values inside the bead due to electrostatic effects (Altier et al. 2016;Puy et al. 2014), but here they are assumed to be equal.

3.4.2.2 Positively charged complexes

In this case, the bead acts as a perfect sink not only for M, but also for ML:

$$J = \frac{D_M}{\delta}c_M + \frac{D_M}{\delta}c_{ML} = \frac{D_M(1+K')}{\delta}c_M \quad (11)$$

As a consequence, due to the direct accumulation of ML, a flux equivalent to the fully labile case ($\xi = 1$) is expected, even if the actual dissociation kinetics was slow. This inability to discriminate between free metal cations and positively charged complexes was already noted in previous works with the equilibrium IET (Fortin and Campbell 1998).

3.4.2.3 Negatively charged complexes

For the extreme case of negative charge and high Boltzmann factor χ, the overall flux of metal to the bead would essentially result from the free metal ions plus some contribution from the dissociation of the complex in the diffusion layer. Dedicated expressions, similar

to those developed in voltammetry (Salvador et al. 2006), could be derived. However, Eqn. (8) still applies rigorously.

3.5 Column models

The modelling of the column considers that the spherical beads receive a flux that may be computed either with Model I or Model II. As the transient period to reach SS for an individual bead has been shown (with Model I) to be much shorter than the typical timescale of the column experiments, we assume in models III and IV that diffusion towards the bead (in the region between r_0 and r_1) is always under SS. This has been called a "diffusional steady state" (dSS) approximation (Galceran and van Leeuwen 2004). Another assumption of the column models is that there is a flat concentration profile of M and ML inside the bead (this is also supported by simulations with Model I, see Fig SI-1). This, again, is consistent with numerical simulation results of a combined particle and film diffusion control of metal uptake in Chelex resins (Quattrini et al. 2017), which indicates that film diffusion is typically the most relevant resistance to mass transfer at short exposure times.

The total concentration of M in the interstices of the column, outside the diffusion boundary layer, at a given height of the column (z) and a given time (t) since the beginning of the experiment, is denoted as $c^{*}_{\mathrm{T,M}}(z,t)$ with a fixed inlet value (at z=0) of $c_{\mathrm{T,M}}$ and an effluent value (at z=$z_{\max}$) of $c^{\mathrm{eff}}_{\mathrm{T,M}}(t)$. Schematic concentration profiles of $c^{*}_{\mathrm{T,M}}(z,t)$ are depicted in Fig SI-4.

3.5.1 Transient model of metal uptake in the column (Model III)

Suitable continuity equations can be derived (see Eqns. (SI-90), (SI-93) and (SI-94)). They involve parameters such as the volume of beads per unit of column length (ρ), the effective bead area per unit of column length (α), the column section (S), the volume

fraction of the column occupied by the flowing solution (ε), and the interstitial velocity of the solution:

$$v = \frac{Q}{S\varepsilon} \quad (12)$$

where Q is the flow rate. ρ was set as the experimental ratio of resin volume over the bed length of the column, while α was computed from the height of the SS plateau as per the equation in Table 2. We applied an effective volume fraction ε of 0.18, the theoretical expectation for close-packing of equal spheres with a slight discounting for the volume fraction represented by the overlapping DBLs around the resin particles.

As seen in Fig 5, Model III reproduces the general shape of the experimental breakthrough curve of Cu-IDA. The values given to the model parameters are gathered in Table 2. r_0 was set as equal to the radius of the bead, while r_1 was fitted. The conditional complexation constant K' was computed directly from the sample composition using Visual MINTEQ (Gustafsson 2016), while k_d was computed according to the Eigen model (Eigen and Wilkins 1965). The model predicts a very short transient period (not experimentally accessible) with a very fast change in the effluent concentration. After the transient period, the effluent concentration becomes approximately constant, corresponding to the attainment of what we identify as the (quasi) steady state. As in DGT, the regime cannot be rigorously termed "steady state" because of the increasing accumulation in the resin, but, for the sake of simplicity in the notation, we will use here the acronym "SS" to indicate this regime. This SS is also consistent with the linearity observed in the Cu-IDA accumulation curve of Fig 2c. For this reason, we suggest labelling this relative stabilisation of the breakthrough curve, just after the transient regime, as the SS plateau.

3.5.2 Steady-state model of metal uptake in the column (Model IV)

As seen in Model III, a quasi SS regime settles for the concentrations of the species in the column at short times. This SS implies an approximate stable flux of metal from solution to the resin (responsible for the initial linear accumulation regime in the accumulation curves) and an approximate constant effluent concentration (the SS plateau). The fundamental equation for column SS Model IV can be derived from Eqn. SI-90; a key property is that ξ is independent from z, as in equation (8). On the other hand, Model IV relaxes the condition of ligand-excess, so that it is also consistent with theoretical lability degrees derived from bead models other than Model II.

As detailed in the next subsections, the differences in mathematical treatment between complexes of different charge are minimal (they only concern the interpretation of ξ, which may be analyzed in a second step).

3.5.2.1 Neutral complexes

As shown in the SI, the ratio between effluent and feed concentrations can be expressed as

$$\ln\frac{c_{\mathrm{T,M}}^{\mathrm{eff,SS}}}{c_{\mathrm{T,M}}} = -\frac{z_{\max}}{z_{\mathrm{char}}} \tag{13}$$

where the superscript “eff, SS” indicates the SS-plateau concentration of the effluent (*i.e.* at z=z_{max}) and

$$z_{\mathrm{char}} = \frac{Q\delta\left(1+K'\right)}{D_{\mathrm{M}}\alpha\left(1+K'\xi\right)} \tag{14}$$

z_{char} can be interpreted as the resin bed length that reduces the feed concentration by a factor e=2.718, so that the shorter z_{char}, the lower will be the effluent total concentration (for a constant z_{max}).

By taking K’=0, previous equations are also valid for experiments where metal is present mostly as the free ion. The ratio of the z_{char} values (computed using Eqn. (13) with the recorded SS plateau concentrations) of two experiments in absence of ligand with

different flow rates (see Fig 6) yielded 0.32, which is reasonably close to the expected value for the ratio of flow rates (0.25), especially if we take into account that δ might decrease with an increasing flow rate.

If we compare two column runs, with and without ligand, one can derive:

$$\frac{\left(\ln\frac{c_{\mathrm{T,M}}^{\mathrm{eff,SS}}}{c_{\mathrm{T,M}}}\right)_{\text{with complex}}}{\left(\ln\frac{c_{\mathrm{T,M}}^{\mathrm{eff,SS}}}{c_{\mathrm{T,M}}}\right)_{\text{absence of ligand}}}=\frac{1+K'\xi}{1+K'} \tag{15}$$

from which the ξ value could be retrieved (see below).

A conclusion of experimental interest is that the use of very small resin sizes and long columns would improve method sensitivity (when using Eqn. (15)), but, on the other hand, small particle sizes can lead to very low ratios of $\frac{c_{\mathrm{T,M}}^{\mathrm{eff,SS}}}{c_{\mathrm{T,M}}}$, with consequent difficulty in determining the height of the plateau.

As shown in the SI, the initial accumulation follows:

$$n^{\mathrm{SS}}=Q\,c_{\mathrm{T,M}}\left[1-\mathrm{e}^{-\frac{z_{\max}}{z_{\mathrm{char}}}}\right]t \tag{16}$$

For small $z_{\max}$ / z_{char} ratios, the previous expression simplifies to

$$n^{\mathrm{SS}}\approx c_{\mathrm{T,M}}\,\frac{D_{\mathrm{M}}\alpha}{\delta}\,\frac{(1+K'\xi)}{(1+K')}\,z_{\max}t \tag{17}$$

which could alternatively be derived from Model II by neglecting any *z*-dependence of the accumulation in the column.

Notice that a very inert system with a large conditional binding constant might yield a very small R_{acc}, which could be mistaken for a situation of sample-resin equilibrium. In principle, these situations could be distinguished by running experiments with varying resin bead volume.

From Eqn. (16),

$$R_{\mathrm{acc}} = Q\, c_{\mathrm{T,M}} \left[1 - \mathrm{e}^{-\frac{z_{\max}}{z_{\mathrm{char}}}} \right] = Q\, c_{\mathrm{T,M}} \left[1 - \frac{c_{\mathrm{T,M}}^{\mathrm{eff,SS}}}{c_{\mathrm{T,M}}} \right] = Q\ c_{\mathrm{T,M}}\ \Xi \tag{18}$$

where Ξ could be called the "system retention degree" (or "apparent column lability degree") which, for fixed total metal and ligand concentrations, increases when the lability degree of the complex increases. This Ξ bears some analogy to the fraction *X* used by some authors (Bowles et al. 2006;Figura and Mcduffie 1979;Procopio et al. 1997). One difference is that Ξ is computed only from the SS plateau concentrations, while *X* is sometimes taken after a fixed volume of sample has gone through the column. Notice that Ξ and *X* can be used even for a case without ligands. For instance, for the case in absence of ligand shown in Fig SI-6 as red square markers, Ξ=0.1. The Ξ values reported in Table 3, computed using

$$\Xi = 1 - \frac{c_{\mathrm{T,M}}^{\mathrm{eff,SS}}}{c_{\mathrm{T,M}}} \tag{19}$$

appear correlated to the lability degree of the complexes according to Model II. Those in Table 4 cannot be usually compared with ξ_{theo} due to the attainment of equilibrium or other reasons. Notice that, for the case of Cu-EDTA, the complex is quite inert at the level of the bead (ξ_{theo} practically 0), but the column depletes the bulk metal concentration and, so, the resulting experimental Ξ-values are in an intermediate range (*e.g.* around 0.5).

Alternatively to Eqn. (15), the lability degree of a complex can be computed the R_{acc} values obtained with and without ligand:

$$\xi = \left(1 + \frac{1}{K'} \right) \frac{\left(\ln\left[1 - \frac{R_{\mathrm{acc}}}{Q c_{\mathrm{T,M}}} \right] \right)_{\text{with complex}}}{\left(\ln\left[1 - \frac{R_{\mathrm{acc}}}{Q c_{\mathrm{T,M}}} \right] \right)_{\text{absence of ligand}}} - \frac{1}{K'} \tag{20}$$

A value of $R_{\mathrm{acc}}=Q\, c_{\mathrm{T,M}}$ would correspond to complete retention of the metal. This ideal situation is approximated quite closely for the cases of metal accumulation in absence of

ligand. A direct consequence, and a possible drawback of this computation method for ξ, is that the denominator of equation (20) may not be estimated with enough accuracy.

3.5.2.2 Positively charged complexes

Expressions of the SS Model IV for $z_{ML}>0$ can be derived from the case of neutral complexes with the additional change of $\xi=1$, whenever the lability degree is involved. So, z_{char} could be computed with Eqn. (13), leading to identical values with or without ligand. No information on the complex kinetics could be extracted from the effluent concentration (Eqn. (15)) or from R_{acc} (Eqn. (16)). R_{acc} will be directly proportional to the total metal concentration, as already observed for Sm-malate and Sm-citrate (Nduwayezu et al. 2016).

3.5.2.3 Negatively charged complexes

As there is practically no penetration of the negative complexes into the beads at the relatively low ionic strength of the experiments, the accumulation will proceed from the flux of free metal, partially supported by the dissociation of the complex within the diffusion layer. This means a very low ξ. However, all the derivations of analytical SS expressions for neutral species (see previous subsection and SI, Model IV) apply rigorously with no other variation.

3.6 The DIET-labile fraction (c_{DIET})

The most recent literature about DGT recognizes that the "concentration" measured with the sampler is not, strictly speaking, the labile fraction, but rather an effective free metal concentration defined as “DGT concentration” (Galceran and Puy 2015;Puy et al. 2016). In analogy, for a set of complexes denoted with index *i* we can introduce a “DIET concentration” defined as:

$$c_{DIET} \equiv c_M \left(1+\sum_i \frac{D_i}{D_M} K_i' \xi_i \right) \quad (21)$$

which is a measure of the effective labile fraction probed by a particular column.

As seen in the SI, c_{DIET} can be evaluated for systems with one complex (assumed to have the same diffusion coefficient as the metal cation), from the SS-plateau concentrations of experiments in presence and absence of ligand (keeping identical conditions such as flow rate, column length, pH, ionic strength and temperature):

$$c_{DIET} = c_{T,M} \frac{\left(\ln \frac{c_{T,M}^{eff,SS}}{c_{T,M}} \right)_{with\ complex}}{\left(\ln \frac{c_{T,M}^{eff,SS}}{c_{T,M}} \right)_{absence\ of\ ligand}} \quad (22)$$

A limitation of this method is that $c_{T,M}^{eff,SS}$ for experiments in absence of ligand may be too close to the limit of detection to be accurately determined. Alternatively, c_{DIET} can be computed from the R_{acc} values:

$$c_{DIET} = c_{T,M} \frac{\left(\ln \left[1 - \frac{R_{acc}}{Q c_{T,M}} \right] \right)_{with\ complex}}{\left(\ln \left[1 - \frac{R_{acc}}{Q c_{T,M}} \right] \right)_{absence\ of\ ligand}} \quad (23)$$

Neither calculation is free from disadvantages, as the same considerations drawn for Eqn. (20) hold here.

3.7 The SS plateau in the breakthrough curve

The presence of the experimental SS plateau was perfectly clear for Cu-IDA at both concentrations of ligand assayed. For instance, in Fig 5, after the sudden initial rise, the effluent concentration stays fixed to approximately 57% of the total sample concentration for at least 1500 s. Given that, all other parameters being equal, the height of the plateau for the experiment in absence of ligand is not higher than 1.7% (see blue squares in Fig SI-6), it can be safely concluded that the IDA complexes have a reduced lability.

Lower plateaus (at about 10% of $c_{T,M}$) can be observed in the curves of metal accumulation in the presence of salicylate or glutamate. Clear SS plateaus have been observed also in the case of Ni-malonate, although at concentrations too low to be safely quantified.

The SS plateau is more apparent when the initial depletion of the metal by the column is not so intense, *i.e.* when $c_{T,M}^{eff}$ is not negligible compared to $c_{T,M}$. For instance, in Fig SI-6, results for small (blue squares) and large (red squares) resin beads obtained with similar flow rates in a Cu solution in absence of ligand can be compared.

Previously, this biphasic behaviour was observed only at low *I* and with trivalent cations (Leguay et al. 2016). This can be explained by considering that the duration of the SS-plateau is related to the time along which the beads act as a perfect sink for M. Increasing the electrostatic partitioning factor χ or the ion charge z_M increases the required jump in concentration at the interface (mathematically: the subtracting terms between round brackets in Eqn. SI-90 vanish), and, as a consequence, the beads tend to behave as perfect sinks for M during longer periods. Also, by comparing the two Ni-only breakthrough curves in Fig 4b, one concludes that the SS plateau is clearer in those cases where R_{acc} is relatively small.

3.8 Retrieval of lability parameters and c_{DIET}

3.8.1 Neutral complexes

Lability degrees for neutral complexes are gathered in Table 3. The theoretical lability degree ξ_{theo} has been computed according to Model II, Eqn. (8), and the required parameters from Table 2. Lability degrees from the SS plateau, Eqn. (15), or from R_{acc}, Eqn. (20), could not be computed for systems with the ligands malate and malonate, but, for the rest of the systems, both values were reasonably close to each other and to the theoretical ξ value. This is also partially due to r_1 having been fitted to 61.6 μm to obtain

such similarity. The agreement between ξ from Eqn. (15) and (20), albeit anticipated, is satisfactory. Given that the experimental concentrations of the SS plateau were not constant, the value of $c_{T,M}^{eff}$ used in Eqn. (15) was taken from the intercept of the linear regression of the first points.

c_{DIET} concentrations for Cu systems with malate or malonate from the SS plateau could not be computed, as the plateau was not observed. As the accuracy of our measurements did not allow us to distinguish the R_{acc} of such systems from the system in absence of ligand, we suggest full lability (as theoretically expected by ξ_{theo}) and estimate $c_{DIET}=c_{T,M}$. For the rest of complexes in Table 3, c_{DIET} values are reasonably in between the fully labile case, when $c_{DIET}=c_{T,M}$ (practically reached for Cu-salicylate), and the completely inert case, when $c_{DIET}=c_M$ (approached by the Cu-IDA system).

3.8.2 Positive complexes

Theoretical lability degrees for the Cu-en system computed with Eqn. (8) yielded a value of 1 (see Table 4). R_{acc} is proportional to the total metal concentration (see Fig SI-8) and, accordingly, the labile fraction c_{DIET} is equal to the total metal concentration. The expected equilibrium accumulation for positive complexes is $\chi^{z_M} c_M + \chi^{z_{ML}} c_{ML}$, much higher than that for neutral complexes (assuming a common bulk free metal concentration).

3.8.3 Negative complexes

In Table 4, the theoretical lability degree is computed with Eqn. (8), even if only the citrate systems are clearly under conditions of excess ligand. For these systems no determinations of ξ are possible due to the fast attainment of equilibrium (see Fig 4). Theoretical ξ values for negative complexes with EDTA are practically 0, as expected from the repulsion of the complex from the resin and the strong ML affinity constant. Consequently, R_{acc} are clearly different from the solutions where the metal is present

almost exclusively as free ion (see Fig 3 or Fig SI-9). The values of ξ retrieved from R_{acc} using Eqn. (20) are slightly negative, which we attribute to experimental uncertainties, but in agreement with a practically totally inert behaviour. The values of c_{DIET} are, accordingly, usually slightly lower than (or almost equal to) the theoretical free fraction. So, in the Cu/Ni-EDTA systems, the use of DIET can effectively determine the free metal ion concentration in the sample.

4. Conclusions

The (practically) constant effluent concentration, described as "SS plateau", seen at short enough times in the breakthrough curves, is associated to a steady-state regime where the beads act as perfect sink for free metal (*i.e.*, they are far away from equilibrium). This (quasi) steady-state regime also explains the initial linear accumulations having a lower slope (*i.e.* slower R_{acc}) than for metal solutions in absence of ligand, or solutions of completely labile complexes (that in the probed systems showed an almost complete retention of the metal, so that R_{acc} approximates $Q\ c_{T,M}$).

One cannot directly relate R_{acc} to the free metal concentration. While this approximation is reasonable in the case of extremely inert complexes (such as Cu/Ni-EDTA), for the majority of the systems assayed here, the rate of metal accumulation includes a contribution from the dissociation of the metal complex.

Model IV is the most useful interpretative framework for short-time exposures in DIET, as it provides a physical overview and simple mathematical expressions to describe the experimentally accessible data. Model III allows the general description of the whole accumulation process from transient period up to attainment of equilibrium *via* numerical simulation. Model II provides the simple expression (8) for the lability degree of the complex (effectively detected by a spherical accumulator), a good estimate of the initial ξ when a judicious value of δ is assumed.

The DIET-labile concentration c_{DIET}, as defined in equation (21), quantifies the labile concentration of a system in DIET measurements using ion exchange resins. Model IV leads to the practical Eqns. (22) and (23) for c_{DIET} computation when assuming common diffusion coefficients of metal and complexes.

If the SS plateau in the breakthough curve is clear enough, the lability degree can be computed –within Model IV- from Eqn. (15) and c_{DIET} from Eqn. (22). Otherwise, one has to resort to R_{acc} by applying Eqn. (20), provided that the difference with the product $Q\,c_{T,M}$ is above the experimental error. The same *caveat* has to be taken into account for computing c_{DIET} with Eqn. (23).

Most of the complexes considered were found to be completely labile, in some cases contrasting with previous voltammetric studies (Agraz et al. 1993). This tendency for DIET to "labilize" the complexes, not dissimilar to the one of DGT (Figura and Mcduffie 1979;Mongin et al. 2011;Puy et al. 2012;van Leeuwen et al. 2005), is a consequence of the complexes penetrating beads with radii being relatively large, in comparison with typical voltammetric reaction layer thicknesses.

The resin bed length has a key role in the retrieved global lability parameter Ξ (see Eqn. (18)). The longer the column, the higher the global lability seen by DIET. This means that each column has an analytical window of labilities, so that future work with columns packed with different amounts of resin and/or different flow rates (Bowles et al. 2006) might prove very useful. For the range of columns analyzed in this work, smaller bed volumes allowed better effluent analysis. Larger amounts of resin improved the limit of detection of the technique (in the eluate analysis) and allowed more frequent sampling of accumulations at short times, but hindered the detection of the SS-plateau regime and rendered R_{acc} practically undistinguishable from $Q\,c_{T,M}$.

The use of the effluent total metal concentration evolution might be limited in natural systems, since the concentrations of the target ions may lie below the limit of quantification. However, it is certainly useful to assess whether a clear SS plateau is present or not in the breakthrough curves

Acknowledgments

The authors gratefully acknowledge support for this research from the Spanish Ministry MINECO (Project CTM2016-78798). Warm thanks to Dr. Peter G.C. Campbell for his very helpful comments. F. Quattrini acknowledges an UdL grant. C. Fortin is supported by the Canada Research Chairs programme. The authors declare no conflicts of interest.

5. References

Agraz R, Sevilla MT, Hernandez L (1993). Copper speciation analysis using a chemically-modified electrode. *Analytica Chimica Acta* **283**, 650-656

Alberti G, Biesuz R, Huidobro C, Companys E, Puy J, Galceran J (2007). A comparison between the determination of free Pb(II) by two techniques: Absence of Gradients and Nernstian Equilibrium Stripping and Resin Titration. *Analytica Chimica Acta* **599**, 41-50 doi:DOI: 10.1016/j.aca.2007.07.055

Altier A, Jimenez-Piedrahita M, Rey-Castro C, Cecilia J, Galceran J, Puy J (2016). Accumulation of Mg to diffusive gradients in thin films (DGT) devices: kinetic and thermodynamic effects of the ionic strength. *Analytical Chemistry* **88**, 10245-10251

Alvarez MB, Malla ME, Batistoni DA (2004). Performance evaluation of two chelating ion-exchange sorbents for the fractionation of labile and inert metal species from aquatic media. *Analytical and Bioanalytical Chemistry* **378**, 438-446

Anderson MA, Morel FMM, Guillard RRL (1978). Growth limitation of a coastal diatom by low zinc ion activity. *Nature* **276**, 70-71

Berggren D (1989). Speciation of aluminum, cadmium, copper, and lead in humic soil solutions - a comparison of the ion-exchange column procedure and equilibrium dialysis. *International Journal of Environmental Analytical Chemistry* **35**, 1-15

Bowles KC, Apte SC, Batley GE, Hales LT, Rogers NJ (2006). A rapid Chelex column method for the determination of metal speciation in natural waters. *Analytica Chimica Acta* **558**, 237-245

Buffle J, Startchev K, Galceran J (2007). Computing steady-state metal flux at microorganism and bioanalogical sensor interfaces in multiligand systems. A reaction layer approximation and its comparison with the rigorous solution. *Physical Chemistry Chemical Physics* **9**, 2844-2855 doi: DOI: 10.1039/b700913e

Cantwell FF, Nielsen JS, Hrudey SE (1982). Free nickel ion concentration in sewage by an ion-exchange column-equilibration method. *Analytical Chemistry* **54**, 1498-1503

Companys E, Galceran J, Pinheiro JP, Puy J, Salaün P (2017). A review on electrochemical methods for trace metal speciation in environmental media. *Current Opinion in Electrochemistry* **3**, 144-162

Companys E, Galceran J, Puy J, Sedo M, Vera R, Antico E, Fontas C (2018). Comparison of different speciation techniques to measure Zn availability in hydroponic media. *Analytica Chimica Acta* **1035**, 32-43

Crémazy A, Leclair S, Mueller K, Vigneault B, Campbell P, Fortin C (2015). Development of an in situ ion-exchange technique for the determination of free Cd, Co, Ni, and Zn concentrations in freshwaters. *Aquatic Geochemistry* **21**, 259-279 doi:WOS:000356246200012

Davison W (2016). Diffusive Gradients in Thin-Films for environmental measurements. Cambridge University Press. (Cambridge, UK)

Eigen M, Wilkins R (1965). *The kinetics and mechanism of formation of metal complexes* in 'Mechanisms of inorganic reactions'. Chap 3, p 55-80 Adv.Chem. Ser. vol. 49, American Chemical Society. DOI:10.1021/ba-1965-0049.ch003

Figura P, McDuffie B (1979). Use of Chelex resin for determination of labile trace-metal fractions in aqueous ligand media and comparison of the method with Anodic-Stripping Voltammetry. *Analytical Chemistry* **51**, 120-125

Figura P, McDuffie B (1980). Determination of labilities of soluble trace-metal species in aqueous environmental-samples by Anodic-Stripping Voltammetry and Chelex column and batch methods. *Analytical Chemistry* **52**, 1433-1439

Fortin C, Campbell PGC (1998). An ion-exchange technique for free-metal ion measurements (Cd^{2+}, Zn^{2+}): Applications to complex aqueous media. *International Journal of Environmental Analytical Chemistry* **72**, 173-194

Fortin C, Campbell PGC (2001). Thiosulfate enhances silver uptake by a green alga: Role of anion transporters in metal uptake. *Environmental Science and Technology* **35**, 2214-2218

Fortin C, Couillard Y, Vigneault B, Campbell PGC (2010). Determination of free Cd, Cu and Zn concentrations in lake waters by *in situ* diffusion followed by column equilibration ion-exchange. *Aquatic Geochemistry* **16**, 151-172

Franklin NM, Rogers NJ, Apte SC, Batley GE, Gadd GE, Casey PS (2007). Comparative toxicity of nanoparticulate ZnO, bulk ZnO, and $ZnCl_2$ to a freshwater microalga (*Pseudokirchneriella subcapitata*): The importance of particle solubility. *Environmental Science and Technology* **41**, 8484-8490 doi:ISI:000251582800046

Galceran J, Puy J, Salvador J, Cecília J, Mas F, Garcés JL (2003). Lability and mobility effects on mixtures of ligands under steady-state conditions. *Physical Chemistry Chemical Physics* **5**, 5091-5100 doi: DOI: 10.1039/b306172h

Galceran J, Puy J, Salvador J, Cecília J, van Leeuwen HP (2001). Voltammetric lability of metal complexes at spherical microelectrodes with various radii. *Journal of Electroanalytical Chemistry* **505**, 85-94 doi:DOI:10.1016/S0022-0728(01)00475-2

Galceran J, van Leeuwen HP (2004). Dynamics of biouptake processes: the role of transport, adsorption and internalisation. In 'Physicochemical kinetics and transport at chemical-biological surfaces. IUPAC Series on Analytical and Physical Chemistry of

Environmental Systems'. (Eds H. P. van Leeuwen, W. Koester) Chap 4. p. 170 (John Wiley: Chichester (UK)).

Galceran J, Puy J (2015). Interpretation of diffusion gradients in thin films (DGT) measurements: a systematic approach. *Environmental Chemistry* **12**, 112-122 doi:http://dx.doi.org/10.1071/EN14068

Gustafsson JP. Visual MINTEQ version 3.1. https://vminteq.lwr.kth.se/download/. 2016.

Herrin RT, Andren AW, Armstrong DE (2001). Determination of silver speciation in natural waters. 1. Laboratory tests of Chelex-100 chelating resin as a competing ligand. *Environmental Science and Technology* **35**, 1953-1958

Leguay S, Campbell PGC, Fortin C (2016). Determination of the free-ion concentration of rare earth elements by an ion-exchange technique: implementation, evaluation and limits. *Environmental Chemistry* **13**, 478-488

Mongin S, Uribe R, Puy J, Cecilia J, Galceran J, Zhang H, Davison W (2011). Key role of the resin layer thickness in the lability of complexes measured by DGT. *Environmental Science and Technology* **45**, 4869-4875 doi:DOI: 10.1021/es200609v

Nduwayezu I, Mostafavirad F, Hadioui M, Wilkinson KJ (2016). Speciation of a lanthanide (Sm) using an ion exchange resin. *Analytical Methods* **8**, 6774-6781

Paquin PR, Gorsuch JW, Apte S, Batley GE, Bowles KC, Campbell PGC, Delos CG, Di Toro DM, Dwyer RL, Galvez F, Gensemer RW, Goss GG, Hogstrand C, Janssen CR, McGeer JC, Naddy RB, Playle RC, Santore RC, Schneider U, Stubblefield WA, Wood CM, Wu KB (2002). The biotic ligand model: a historical overview. *Comparative Biochemistry and Physiology C-Toxicology & Pharmacology* **133**, 3-35 doi:ISI:000178949100002

Peijnenburg WJGM, Teasdale PR, Reible D, Mondon J, Bennett WW, Campbell PGC (2014). Passive sampling methods for contaminated sediments: State of the science for metals. *Integrated Environmental Assessment and Management* **10**, 179-196 doi:WOS:000333241900005

Pesavento M, Alberti G, Biesuz R (2009). Analytical methods for determination of free metal ion concentration, labile species fraction and metal complexation capacity of environmental waters: A review. *Analytica Chimica Acta* **631**, 129-141 doi:ISI:000262585800002

Pesavento M, Sturini M, D'Agostino G, Biesuz R (2010). Solid phase extraction of copper(II) by fixed bed procedure on cation exchange complexing resins. *Journal Of Chromatography A* **1217**, 1208-1218

Procopio JR, Viana MDM, Hernandez LH (1997). Microcolumn ion-exchange method for kinetic speciation of copper and lead in natural waters. *Environmental Science and Technology* **31**, 3081-3085

Puy J, Galceran J, Cruz-Gonzalez S, David CA, Uribe R, Lin C, Zhang H, Davison W (2014). Metal accumulation in DGT: Impact of ionic strength and kinetics of

dissociation of complexes in the resin domain. *Analytical Chemistry* **86**, 7740-7748 doi:10.1021/ac501679m

Puy J, Galceran J, Rey-Castro C (2016). Interpreting the DGT measurement: speciation and dynamics. In 'Diffusive Gradients in Thin-Films for environmental measurements'. (Eds W. Davison) pp. 93-122 (Cambridge University Press: Cambridge).

Puy J, Uribe R, Mongin S, Galceran J, Cecilia J, Levy J, Zhang H, Davison W (2012). Lability criteria in Diffusive Gradients in Thin films. *Journal of Physical Chemistry A* **116**, 6564-6573 doi: 10.1021/jp212629z

Puy J, Galceran J (2017). Theoretical aspects of dynamic metal speciation with electrochemical techniques. *Current Opinion in Electrochemistry* **1**, 80-87 doi:http://www.sciencedirect.com/science/article/pii/S2451910316300382

Quattrini F, Galceran J, David CA, Puy J, Alberti G, Rey-Castro C (2017). Dynamics of trace metal sorption by an ion-exchange chelating resin described by a mixed intraparticle/film diffusion transport model. The Cd/Chelex case. *Chemical Engineering Journal* **317**, 810-820

Rowell JA, Fillion MA, Smith S, Wilkinson KJ (2018). Determination of the speciation and bioavailability of samarium to *Chlamydomonas reinhardtii* in the presence of natural organic matter. *Environmental Toxicology and Chemistry* **37**, 1623-1631

Salvador J, Puy J, Cecilia J, Galceran J (2006). Lability of complexes in steady state finite planar diffusion. *Journal of Electroanalytical Chemistry* **588**, 303-313 doi:DOI: 10.1016/j.jelechem.2006.01.005

Sunda WG (1984). Measurement of manganese, zinc and cadmium complexation in seawater using Chelex ion-exchange equilibria. *Marine Chemistry* **14**, 365-378

Tantra R, Bouwmeester H, Bolea E, Rey-Castro C, David CA, Dogne JM, Jarman J, Laborda F, Laloy J, Robinson KN, Undas AK, van der Zande M (2016). Assessing suitability of analytical methods to measure solubility for the purpose of nano-regulation. *Nanotoxicology* **10**, 173-184 doi:10.3109/17435390.2015.1038661

Temminghoff EJM, Plette ACC, van Eck R, van Riemsdijk WH (2000). Determination of the chemical speciation of trace metals in aqueous systems by the Wageningen Donnan Membrane Technique. *Analytica Chimica Acta* **417**, 149-157 doi:ISI:000088230500004

Uribe R, Mongin S, Puy J, Cecilia J, Galceran J, Zhang H, Davison W (2011). Contribution of partially labile complexes to the DGT metal flux. *Environmental Science and Technology* **45**, 5317-5322 doi:10.1021/es200610n

van Leeuwen HP, Town RM, Buffle J, Cleven R, Davison W, Puy J, van Riemsdijk WH, Sigg L (2005). Dynamic speciation analysis and bioavailability of metals in aquatic systems. *Environmental Science and Technology* **39**, 8545-8585

Vera R, Fontàs C, Galceran J, Serra O, Anticó E (2018). Polymer inclusion membrane to access Zn speciation: Comparison with root uptake. *Science of the Total Environment*

622–623, 316-324
doi:https://www.sciencedirect.com/science/article/pii/S0048969717333739

Wen LS, Jiann KT, Santschi PH (2006). Physicochemical speciation of bioactive trace metals (Cd, Cu, Fe, Ni) in the oligotrophic South China Sea. *Marine Chemistry* **101**, 104-129

Zhao CM, Campbell PGC, Wilkinson KJ (2016). When are metal complexes bioavailable? *Environmental Chemistry* **13**, 425-433 doi:WOS:000377043800002

Tables

Table 1. Models developed in this work to describe the analyte accumulation by the resin. The models are categorised according to the regimes they assume (only steady-state or all regimes) and the geometry of the system (single spherical resin bead or whole packed column). The table also reports the applications of each model.

	Including all regimes (transient, SS, equilibrium, etc.)	**Steady-state regime only**
Individual resin bead	Model I It shows that steady state is reached almost instantaneously	Model II It allows estimating the lability degree (ξ), Eqn. (8)
Whole column	Model III It shows that the initial plateau in the breakthrough curves and R_{acc} are related to a steady-state regime	Model IV Practical model to interpret DIET results (Eqns. (15), (20), (22) and (23)).

Table 2. Parameter values used in the description of the accumulation and breakthrough curves of neutral complexes of Cu.

Parameter	Value	Source
z_{max} (m)	$6\pm1\times10^{-3}$	direct measurement (average over 6 columns)
	1×10^{-3}	direct measurement
S (m^2)	3.85×10^{-5}	direct measurement
	1.26×10^{-5}	
r_0 (m)	1.12×10^{-4} (50-100 Mesh)	from nominal average size of the beads
	5.60×10^{-5} (100-200 Mesh)	
	2.80×10^{-5} (200-400 Mesh)	
ε	0.18	70% of the value given by the close packing of spheres of equal volume
ρ (m^2)	1.80×10^{-5}	$\rho = \frac{V_R}{z_{max}}$, where V_R is the volume of the resin matrix
	1.10×10^{-5}	
α (m)	0.234 (50-100 Mesh, S)	$\alpha = -\frac{\delta Q \ln \frac{c_{T,M}^{eff,SS}}{c_{T,M}}}{D_M z_{max}}$ (Eqn. (SI-105))
	0.499 (100-200 Mesh, S)	
	0.203 (200-400 Mesh, S)	
D_M ($m^2\ s^{-1}$)	7.14×10^{-10} (Cu) 6.61×10^{-10} (Ni)	from literature (values at 25ºC)
δ (m)	10×10^{-6} (50-100 Mesh) (flow rate 7.5×10^{-8} m^3 s^{-1})	fitted
	7×10^{-6} (100-200 Mesh) (flow rate 7.5×10^{-8} m^3 s^{-1})	
	5×10^{-6} (200-400 Mesh) (flow rate 7.5×10^{-8} m^3 s^{-1})	
	10×10^{-6} (200-400 Mesh) (flow rate 1.9×10^{-8} m^3 s^{-1})	

Table 3. Compilation of studied systems corresponding to neutral complexes. All the experiments were carried out with the same columns packed with ∼0.1 g of Dowex 50x4 100-200 mesh. For computations, the average bead radius is r_0=5.6×10^{-5} m, the diffusion layer thickness δ=7×10^{-6} m, the section of the column S=3.85×10^{-5} m^2 and the length of the column z_{max}=6.0×10^{-3} m.

System	$c_{T,L}$ **(mol L^{-1})**	$c_{T,M}$ **(mol L^{-1})**	ξ_{theo} **according to Model II, Eqn.** (8)	ξ **from** R_{acc} **according to Model IV Eqn.** (20)	ξ **from effluent concentration according to Model IV Eqn.** (15)	z_{char} **(m)** (14)	Ξ (19)	c_{DIET} **(mol L^{-1})** (22)	c_{DIET} **(mol L^{-1})** (23)	c_M **(mol L^{-1})Visual MINTEQ**
Cu-Glutamate	5×10^{-4}	2.34×10^{-7}	0.70	0.86	0.63	2.3×10^{-3}	0.92	1.49×10^{-7}	2.02×10^{-7}	3.09×10^{-9} [a]
	5×10^{-7}	2.34×10^{-7}	0.17	0.10	0.05	1.0×10^{-2}	0.44	3.37×10^{-8}	4.35×10^{-8}	2.47×10^{-8}
Cu-IDA	5×10^{-6}	2.38×10^{-7}	0.16	0.10	0.08	1.8×10^{-2}	0.28	1.97×10^{-8}	2.44×10^{-8}	1.58×10^{-9}
	1.5×10^{-4}	2.79×10^{-7}	1.00	≈1[b]	---[c]	---[c]	≈1	---[c]	≈c_{TM}[b]	7.81×10^{-8}
	1×10^{-3}	2.49×10^{-7}	1.00	≈1[b]	---[c]	---[a]	≈1	---[c]	≈c_{TM}[b]	1.49×10^{-8}
Cu-Malate	5×10^{-3}	2.54×10^{-7}	1.00	---[d]	---[c]	---[c]	≈1	---[c]	---[e]	3.83×10^{-9}
Cu-Malonate	1×10^{-4}	2.49×10^{-7}	0.99	≈1[b]	---[c]	---[c]	≈1	---[c]	≈c_{TM}[b]	8.55×10^{-10}
Cu-Salicylate	5×10^{-3}	2.34×10^{-7}	1.00[d]	≈1[b]	0.95	1.6×10^{-3}	≈1	2.23×10^{-7}	≈c_{TM}[b]	1.60×10^{-8}
	5×10^{-4}	2.46×10^{-7}	0.86	≈1[b]	---[f]	6.6×10^{-3}	≈1	---[f]	≈c_{TM}[b]	6.94×10^{-8}
Ni-Malonate	1×10^{-3}	2.39×10^{-7}	0.86	≈1[b]	---[f]	2.1×10^{-3}	≈1	---[f]	≈c_{TM}[b]	4.12×10^{-8}

[a] The positively charged species Cu-HGlutamate$^+$, which accumulates in the resin along with the free metal, is present at a bulk concentration equal to 2.36×10^{-9} mol L^{-1}

[b] The initial slope of the accumulation curve (R_{acc}) practically coincides with the one of metal in absence of ligand

[c] The plateau corresponding to the Steady State could not be clearly observed in the breakthrough curve

[d] ξ computed assuming that the reactive species is LH$^-$, instead of L^{2-} as in the other cases

[e] The almost instantaneous attainment of equilibrium does not allow determining R_{acc}

[f] The equation cannot be implemented, as we do not have results of Ni in absence of ligands. Ni-R_{acc} has been assumed as the one of Cu

Table 4. Compilation of studied systems corresponding to charged complexes. All the experiments were carried out with columns packed with ∼0.01 g of Dowex 50x2 resin, 200-400 mesh. The average r_0 is 2.8×10^{-5} m, δ is 5×10^{-6} m, S is 1.96×10^{-5} m^2 z_{max} is 1.0×10^{-3} m.

System	Complex charge	$c_{T,L}$ (mol L^{-1})	$c_{T,M}$ (mol L^{-1})	ξ_{theo} Model II Eqn. (8)	ξ from equation (20)	Ξ (19)	c_{DIET} (mol L^{-1}) (23)	c_M (mol L^{-1}) Visual MINTEQ
Cu-Citrate	-1	5.00×10^{-5}	2.50×10^{-7}	0.78	---[a]	≈0[a]	---[a]	1.51×10^{-9}
Cu-EDTA	-2	6.30×10^{-8}	2.42×10^{-7}	0.00[b]	≈0[c]	0.79	1.61×10^{-7}	1.73×10^{-7}
		1.25×10^{-7}	2.33×10^{-7}	0.00[b]	≈0[c]	0.56	8.25×10^{-8}	1.04×10^{-7}
		1.88×10^{-7}	2.50×10^{-7}	0.00[b]	≈0[c]	0.30	3.83×10^{-8}	5.98×10^{-8}
Cu-en	+2	1.00×10^{-6}	2.50×10^{-7}	1.00[b]	≈1[d]	≈1	≈c_{TM}[d]	1.81×10^{-7}
		2.70×10^{-6}	2.50×10^{-7}	1.00[b]	≈1[d]	≈1	≈c_{TM}[d]	1.25×10^{-7}
		7.80×10^{-6}	2.50×10^{-7}	1.00[b]	≈1[d]	≈1	≈c_{TM}[d]	6.18×10^{-8}
Ni-Citrate	-1	5.00×10^{-4}	2.44×10^{-7}	0.003	---[a]	≈0[a]	---[a]	8.39×10^{-10}
Ni-EDTA	-2	5.93×10^{-8}	2.37×10^{-7}	0.00[b]	≈0[c]	0.83	1.81×10^{-7}	1.76×10^{-7}
		1.33×10^{-7}	2.65×10^{-7}	0.00[b]	≈0[c]	0.48	7.56×10^{-8}	1.31×10^{-7}
		1.94×10^{-7}	2.59×10^{-7}	0.00[b]	≈0[c]	0.33	4.48×10^{-8}	6.44×10^{-8}

[a] The equilibrium is attained almost instantaneously

[b] The system was not under ligand excess conditions, so Model II does not hold strictly

[c] As a consequence of uncertainties on the slopes and on K', Eqn. (20) give slightly negative values of ξ

[d] The slope of the accumulation curve (R_{acc}) practically coincides with the one of the metal in absence of ligand

Figures

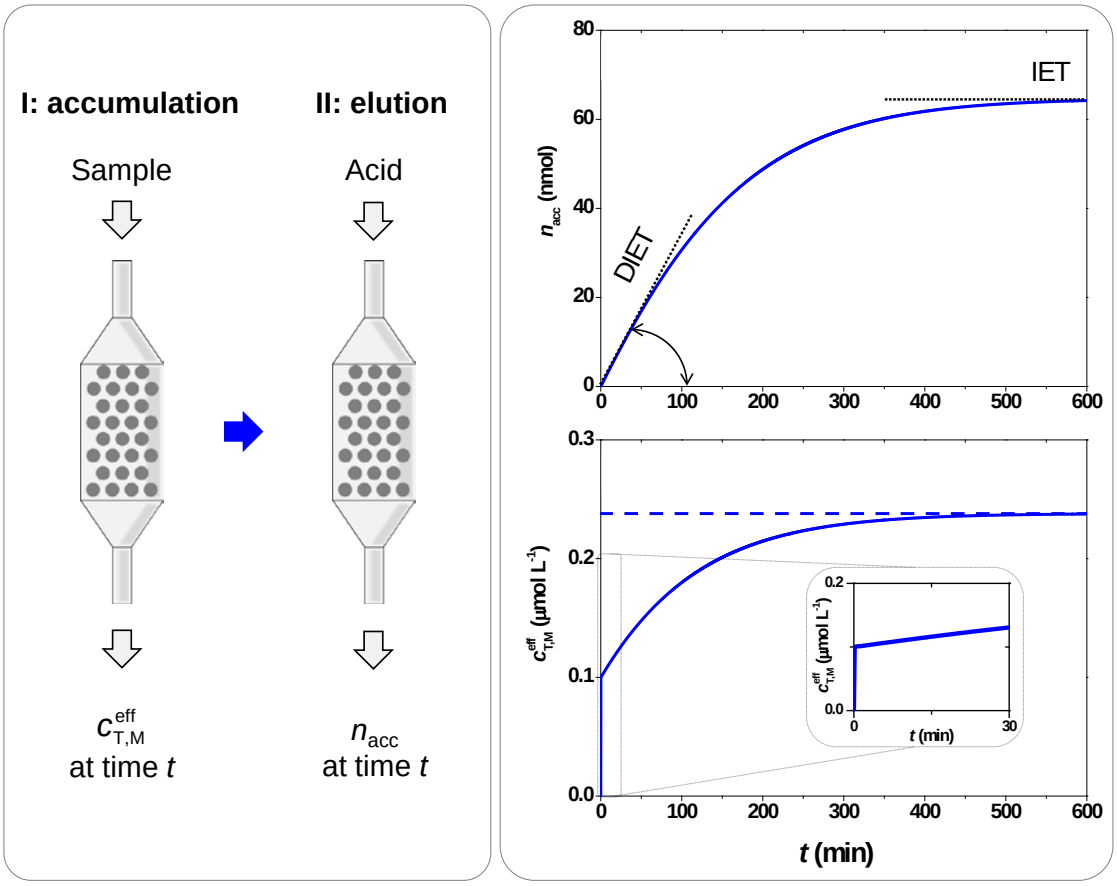

Fig 1: Panel a: Schematic representation of the setup of DIET (dynamic mode) and IET (equilibrium mode). In the accumulation step the sample is flushed through the resin-packed column, while in the elution step the metal accumulated in the resin is recovered by flushing an acidic solution through the column. Panel b: accumulation curve of a metal in the resin. The labels indicate the operational regions of DIET (dynamic mode) and IET (equilibrium mode) as well as R_{acc}, the rate of accumulation (or initial slope). Panel c: breakthrough curve corresponding to the accumulation curve in Panel b. The dashed line stands for the expected effluent concentration at equilibrium. The inset highlights the initial part of the curve showing the (quasi) steady-state regime.

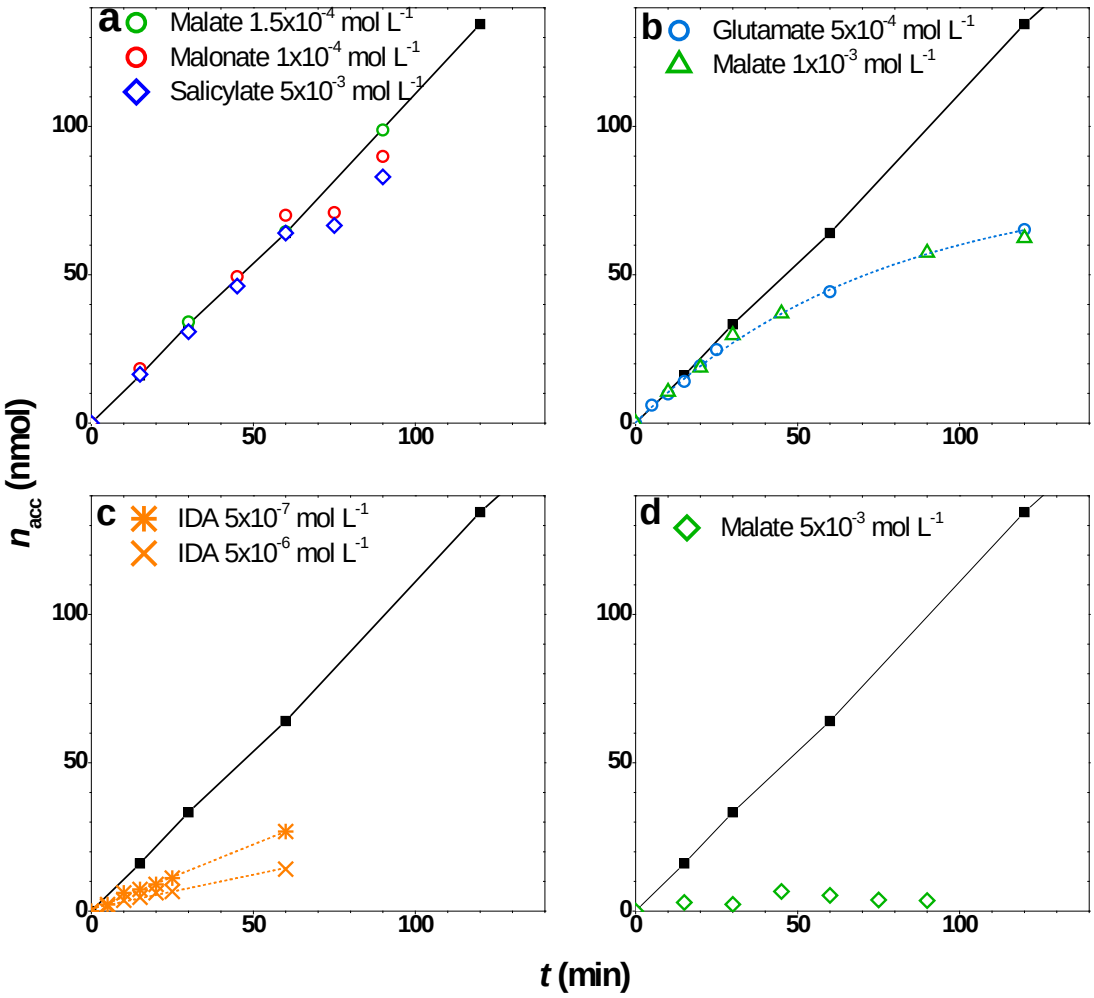

Fig 2: Cu accumulation curves in columns of Dowex 50x4 (100-200 mesh) resin, corresponding to samples containing the same (nominal) total Cu concentration and varying amounts of ligands forming neutral complexes. Panel a: complexes with R_{acc} equal to that of a solution in absence of ligand (at all recorded exposure times). Panel b: complexes with initial R_{acc} (at short exposure times) equal to that of a solution in absence of ligand, but diverging for longer times. Panel c: complexes with R_{acc} smaller than that of the solution in absence of ligand (i.e. just Cu). Panel d: complexes that equilibrate almost instantaneously with the resin. In each case, the accumulation curve in absence of ligands is shown for comparison purposes. Parameters: m_{resin}=100 mg; flow rate, Q=4.5 mL min^{-1}; $c_{T,Cu} \simeq 2.5\times10^{-7}$ mol L^{-1}. See Table 3 for composition details. The dotted lines in panels b and c are a guide to the eye.

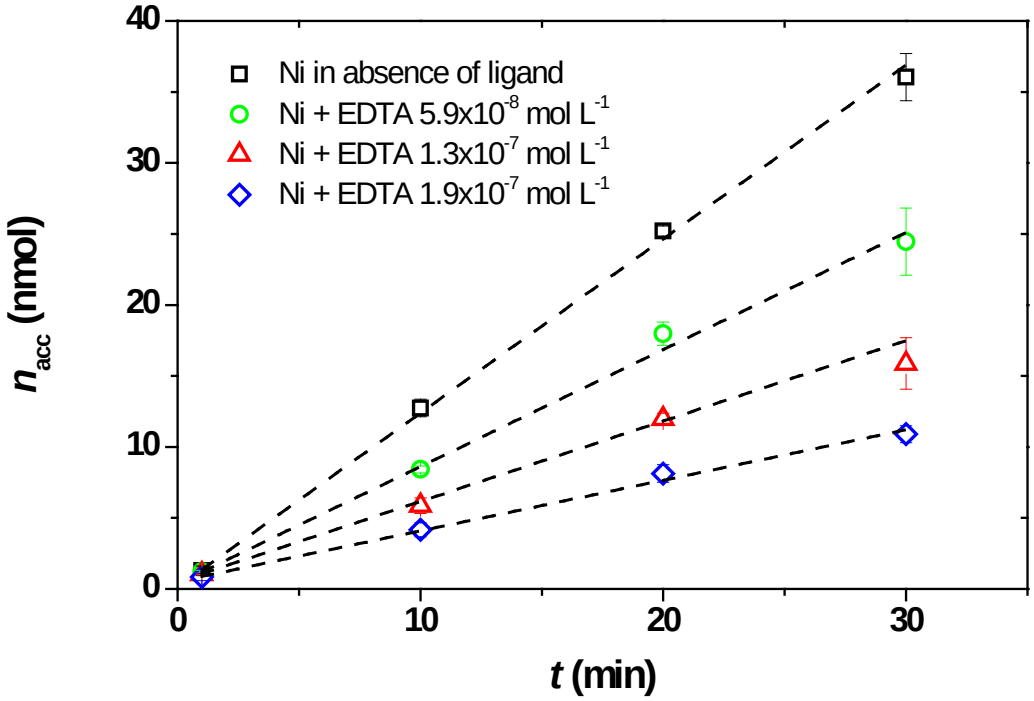

Fig 3: Accumulation curves of Ni in Dowex 50x4 (200-400 mesh) in presence of three different concentrations of EDTA exhibiting accumulation rates proportional to the free ion concentration. Each series corresponds to a different c_{Ni}, reported in the legend. The points stand for the average of three independent columns, while the dashed lines were given by the linear regression over all the data points $c_{T,Ni}=2.5\times10^{-7}$ mol L^{-1}, $Q=4.5$ mL min^{-1}.

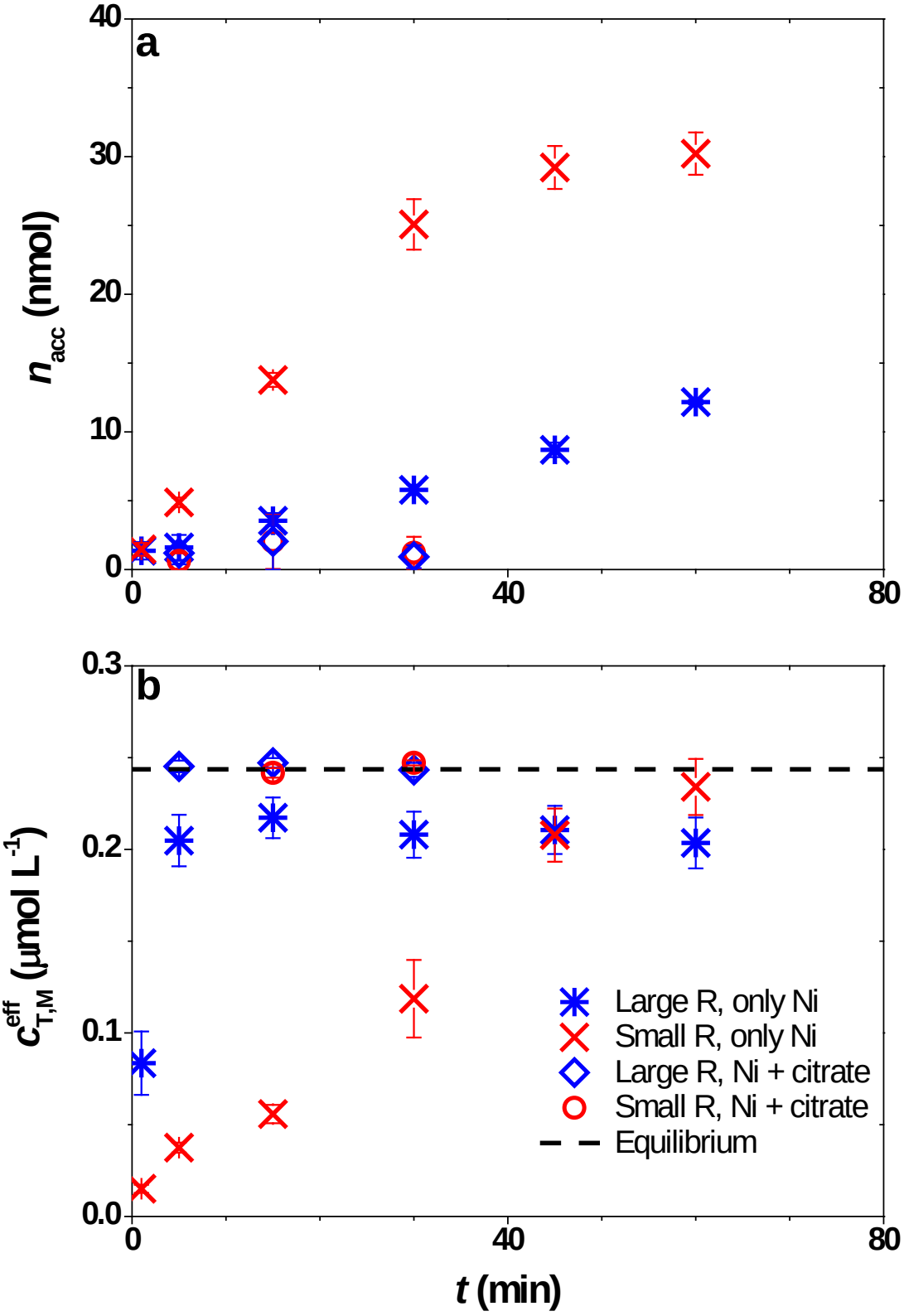
a
b
n_{acc} (nmol)
$c^{eff}_{T,M}$ (µmol L^{-1})
t (min)
0
10
20
30
40
0
40
80
0.0
0.1
0.2
0.3
Large R, only Ni
Small R, only Ni
Large R, Ni + citrate
Small R, Ni + citrate
Equilibrium

Fig 4: Accumulation of Ni, in presence and in absence of a competing ligand (citrate) on Dowex resin beads of different sizes ("large R": Dowex 50x8 50-100 mesh; "small R": Dowex 50x2 200-400 mesh). Panel a: accumulation curves; Panel b: breakthrough curves. Blue stars: no ligand added, resin 50-100 Mesh; red crosses: no ligand added, resin 200-400 Mesh; blue diamonds: citrate 5×10^{-4} mol L^{-1}, resin 50-100 Mesh; red circles: citrate 5×10^{-4} mol L^{-1}, resin 200-400 Mesh. In panel b the dashed line stands for the eventual equilibrium value. The experiments in absence of ligand were performed in triplicate, while the experiments in presence of citrate were performed in duplicate. In this latter case, the error bars are hidden by the symbols.

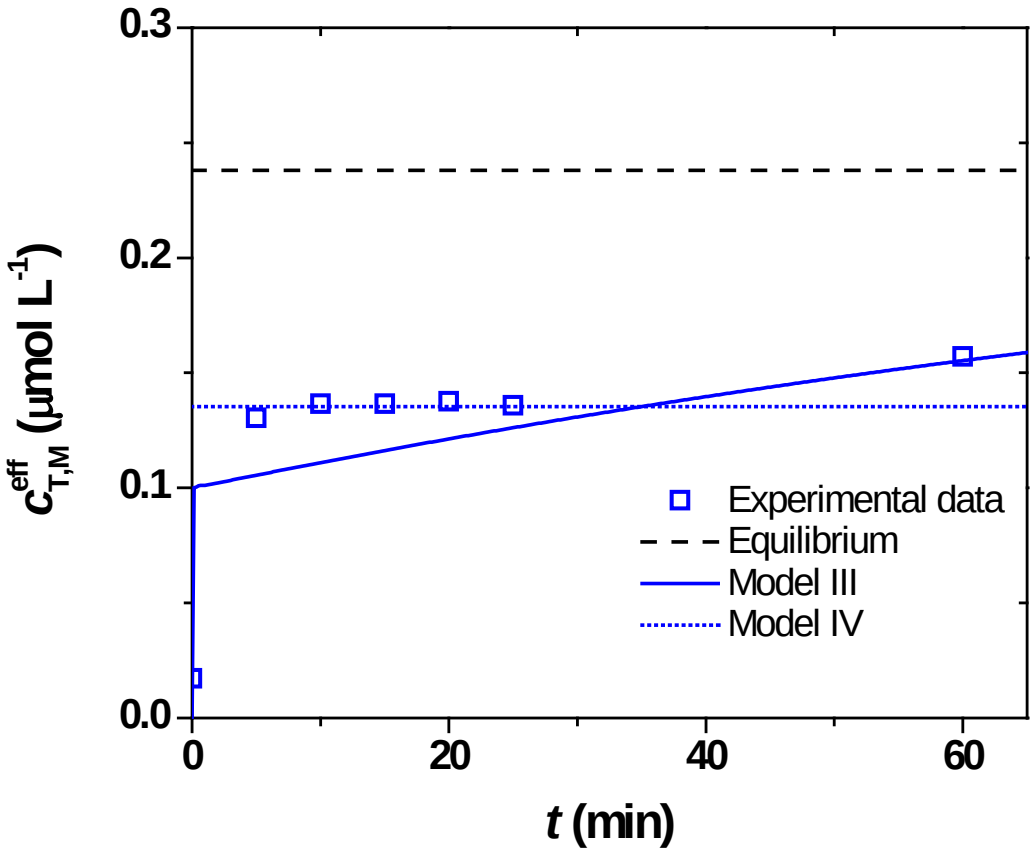

Fig 5: Breakthrough curve of Cu in presence of IDA , with $c_{T,IDA}=5\times10^{-7}$ mol L^{-1}. Markers: experimental data; continuous blue line: Model III; dotted blue line: Model IV; dashed black line: equilibrium value. $c_{T,Cu}=2.47\times10^{-7}$ mol L^{-1}, Q=4.5 mL min^{-1}.

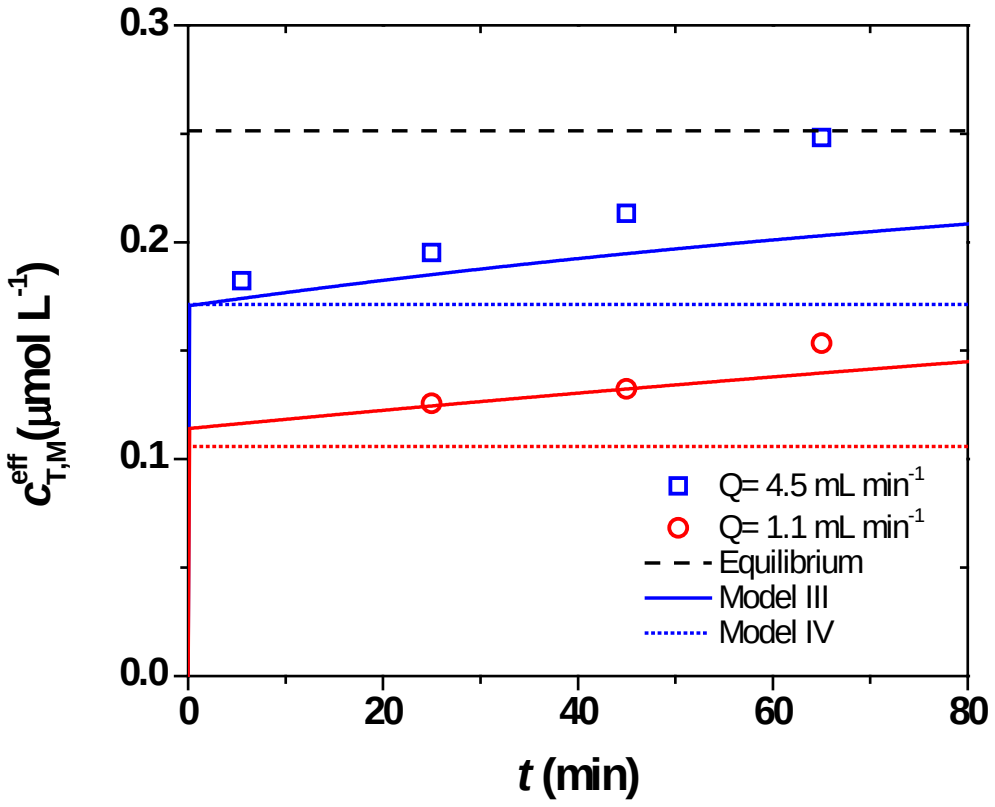

Fig 6: Impact of flow rate on breakthrough curves of Cu in absence of ligand, with $c_{T,M}$=2.5×10^{-7} mol L^{-1}, Q=4.5 (blue) and 1.1 (red) mL min^{-1}. Markers: experimental data; continuous lines: Model III; dotted lines: Model IV; dashed black line: equilibrium value.